ANL-6731

ANL-6731

Argonne National Laboratory

GALVANOMAGNETIC PROPERTIES OF URANIUM MONOSULFIDE

by

Casimir W. Kazmierowicz

ANL-6731
Chemistry
(TID-4500, 21st Ed.)
AEC Research and
Development Report

ARGONNE NATIONAL LABORATORY
9700 South Cass Avenue
Argonne, Illinois 60440

GALVANOMAGNETIC PROPERTIES OF URANIUM MONOSULFIDE

by

Casimir W. Kazmierowicz

Solid State Science Division

Based on a Thesis
Submitted in Partial Fulfillment of the
Requirements for the Degree of
Master of Science in Physics
in the Graduate School of
Illinois Institute of Technology

June 1963

Operated by The University of Chicago
under
Contract W-31-109-eng-38
with the
U. S. Atomic Energy Commission

TABLE OF CONTENTS

LIST OF FIGURES

LIST OF TABLES

GALVANOMAGNETIC PROPERTIES OF URANIUM MONOSULFIDE

by

Casimir W. Kazmierowicz

CHAPTER I

HISTORICAL INTRODUCTION

Incentives for This Research

It has been discovered recently that uranium monosulfide (US) is ferromagnetic below 180°K.[1]* In view of this fact and because of the growing interest in this and similar materials from the standpoint of thermoelectric processes, a study of the galvanomagnetic properties seems appropriate. Such a study was undertaken with the following primary objectives.

The first objective was to compare the Hall effect, resistivity, and magnetoresistance of US with the equivalent properties of other ferromagnetic materials. Secondly, but more importantly, it was hoped that the results of this study will contribute to the knowledge of the nature of the conduction process in US. The following two sections are offered as a brief history of the galvanomagnetic properties of the common ferromagnetic materials.

The Resistivity and Magnetoresistance of Ferromagnetic Materials

The resistivity ρ of a ferromagnetic material is abnormally low at temperatures below its Curie point.[2] Becker and Döring[3] have shown this by comparing the resistivities of nickel and palladium. If the resistivities of these elements are plotted as a function of temperature in such a way that they coincide at the Curie point, θ, of nickel, the two curves obtained are nearly the same at temperatures above θ. At θ the curves separate and the nickel curve is lower at lower temperatures. Mott[4] has offered an explanation of this behavior on the basis of the band picture of the distribution of electrons in the atoms of the iron group.

According to Mott, conduction takes place mainly by electrons in the s-band. These are disturbed by frequent transitions to the unfilled d-bands and, as a result, the resistivity of nickel is high as compared with copper, in which the d-bands are filled. When ferromagnetism occurs,

*For all numbered references, see bibliography.

one of the two d-bands is filled and transitions to it do not occur. This results in a decrease in scattering and, as a result, the resistivity of nickel below the Curie point is lower than that of an element like palladium, which also has unfilled inner shells but is not ferromagnetic.

The electrical resistivity of a ferromagnetic material changes when it is magnetized.[2] This magnetoresistance is not always positive (indicating an increase in resistivity) as it usually is for nonferromagnetics. In low fields the longitudinal effect $\Delta\rho_{\parallel}$ (when the magnetization is parallel to the current) is positive and the transverse effect $\Delta\rho_{\perp}$ (when the magnetization is at right angles to the current) is negative. Above saturation, both magnetoresistances are negative and depend linearly on the applied field. The normal increase in resistivity observed in most materials is present in ferromagnetics, although it is a much smaller effect than the abnormal decrease and can be detected only at very low temperatures.

The negative magnetoresistance above saturation is accounted for by Mott's theory. Above saturation, the magnetization can slowly increase; as a result, fewer transitions of s-band electrons can occur and, consequently, the resistivity is decreased.

There is a sharp minimum in the plot of magnetoresistance versus temperature which occurs at the Curie point. Gerlach[5] points out that the shape of this curve may be useful in determining the Curie point. The minimum at the Curie point is consistent with Mott's theory in that the increase in magnetization above saturation is very pronounced near the Curie point.

The Hall Effect in Ferromagnetic Materials

The Hall effect in ferromagnetic materials is studied in the same way that it is in nonferromagnetic materials. If a current is passed through a specimen and a magnetic field is applied perpendicular to this current, a transverse emf is found, which is referred to as the Hall emf.

It has been known for a long time that the Hall effect in ferromagnetic materials is fundamentally different from that found in nonferromagnetic materials. The main differences are related to the way that the Hall emf varies with applied field and temperature. From studies of the Hall effect in iron, cobalt, and nickel,[6-11] it was found that the Hall emf in these materials consists of a sum of two terms. The first term, called the ordinary Hall effect, is proportional to the applied field. The second term, called the extraordinary Hall effect, is proportional to the intensity of magnetization.

Pugh[8] was the first to suggest the following empirical equation:

$$\epsilon = - E_H/ib = R_0H + R_1I \quad , \qquad (1)$$

where E_H is the Hall emf, i is the current density, b is the width of the plate between Hall probes, ϵ is the Hall electric field per unit current density, R_0 is the ordinary Hall coefficient, H is the magnetic field, R_1 is the extraordinary Hall coefficient, and I is the intensity of magnetization.

Using plate-shaped samples of nickel, Pugh, Rostoker, and Schindler[10] showed that above saturation, where I in equation (1) is equal to the saturation magnetization I_s, the Hall emf is indeed linear with H. The slope of the straight line yielded a value of R_0. The intercept of this line with the axis H = 0 and the separately determined saturation magnetization of the nickel determined the value of R_1. The values found at 20.3°C were $R_0 = - 0.611 \times 10^{-12}$ v-cm/amp-oe and $R_1 = - 74.9 \times ^{-12}$ v-cm/amp-oe.

The ordinary Hall coefficients of the ferromagnetic elements were found to be of the same order of magnitude as those of the nearest-neighbor nonferromagnetic elements in the periodic table. Except for an anomalous behavior near the Curie point,[12] the value of R_0 is independent of temperature and has the same value above and below the Curie point. The extraordinary Hall coefficients, on the other hand, were found to be considerably higher in magnitude than the ordinary ones and quite dependent on temperature. Thus, R_1 increases steadily with temperature up to the Curie point and diminishes rapidly to zero above the Curie point.

Karplus and Luttinger[13] have predicted, on the basis of spin-orbit interaction of polarized conduction electrons, that the extraordinary Hall coefficient should be proportional to the square of the ordinary resistivity. They also predict that the proportionality constant should be insensitive to temperature and impurity content, and should be of the order of unity. Kooi[14] and others[15,16] have found that the experimental results for iron and its alloys are in very good agreement with this prediction. Measurements of nickel and its alloys agree at least qualitatively.

Description and Preparation of Uranium Monosulfide

Uranium monosulfide is one of a rather large number of known compounds of formula MS, in which M may be a metal in any group of the Periodic Table except IA and IIIB.[17] There has been recent interest in the high-temperature properties of US. Its high melting point makes it suitable for use as a fuel in a nuclear reactor. Because of the high thermoelectric figure of merit for US, the possibility of its use in thermoelectric devices is being investigated. Table 1 indicates some of its physical properties.

Table 1. Physical Properties of US

Appearance	Bright metallic luster, gold or silver
Melting Point	2462^{+30}_{-5}°C
Crystal Structure	Cubic (NaCl-type) $a_0 = 5.4903 \pm 0.002$ Å
Solid Solution	Probably $0.96 \pm 0.01 < S/U < 1.01 \pm 0.01$
Vacuum Behavior	Congruent vaporization to U + S + US_2
Resistivity at 25°C	$100 \pm 30\mu$ ohm-cm
Theoretical Density	10.87 g/cc

Uranium monosulfide can be prepared in various ways. The following method of preparation, used by Cater,[17] is most common. Pure uranium metal is reacted with hydrogen to yield UH_3. The UH_3 is decomposed to give finely divided uranium metal. Reaction of this fine powder with H_2S gives a mixture of metal and higher sulfides. This mixture is heated to a temperature in the range of 1800-2100°C in a tungsten crucible in vacuum to produce sintered, crystalline uranium monosulfide.

CHAPTER II

METHOD OF APPROACH

Sample Preparation

The material used in this study was polycrystalline US which had been prepared by the method outlined in Chapter I. Chemical analyses of the samples are given in Table 2 along with other pertinent information. The examination of a polished section of Sample P-109 indicated that most of the insoluble residue consisted of UOS. Most of the data reported in this paper were obtained from measurements with Samples P-72 and P-109.

Table 2. Typical Analyses of Samples Used

Sample Number	Heat Treatment	% Insoluble Residue	S/U Soluble	Density, g/cc	Remarks
P-1	Sintered	3.8	1.20	-	-
P-25	Arc Melted	4.0 ± 1.0	1.13	-	Yielded irreproducible electrical measurements.
P-72	Sintered	1.22	0.98	9.57	The chemical analysis was made after all electrical measurements were obtained.
P-109	Sintered	3.63	1.02	9.53	A polished section was studied.

The samples were machined from cylindrical pellets to give the shape illustrated in Figure 1(a). The average length of the samples was 10 mm, the width was 3 mm, and the thickness was 1 mm. Tabs B and C were 5 mm apart. Hall emfs were measured across tabs A and B, resistivity and magnetoresistance across tabs B and C.

Apparatus Used to Make Galvanomagnetic Measurements

Numerous methods of holding the sample and attaching leads to it were tried. The method finally adopted is illustrated in Figure 1(b). This method allowed for an expansion or contraction of the sample due to temperature changes without any appreciable strain on it. The current leads consisted of large copper plates clamped to each end of the sample. To assure good electrical and thermal contact, pieces of platinum foil were wrapped around the ends of the sample before it was clamped in the copper. Large current leads were chosen to reduce temperature gradients. The potential leads were 5-mil platinum wires which were attached to the tabs of the sample with conducting silver paint to assure good contact and to

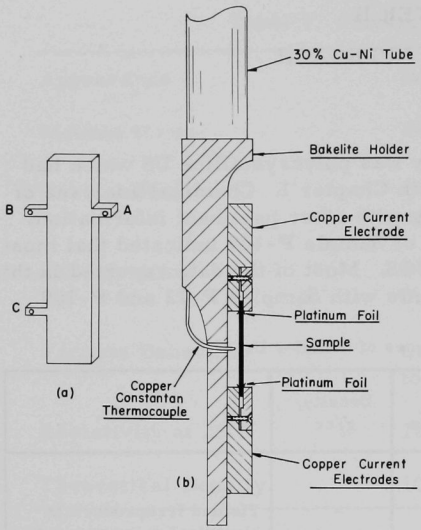

Figure 1. (a) Sample Geometry, (b) Sample Holder Used in Making Electrical Measurements

reduce contact potentials. This type of sample holder provided a means of cycling the sample through a wide range of temperatures without sacrificing reproducibility in the measurements.

The sample holder was attached to one end of a 30 per cent Cu-Ni tube, which made it possible to position the sample in a long, narrow metal Dewar flask, the bottom of which was fixed in the pole gap of a magnet. The smallest pole gap for which the magnet was calibrated was 0.640 in. long and 2.0 in. in diameter. The maximum field attained with this arrangement was 20 koe. Larger pole gaps were used with glass Dewars at the expense of a decreased maximum field.

A standard dc method was used to make the galvanomagnetic measurements. The primary sample current was maintained by means of a constant-current regulator. Most of the measurements were made with a primary current of 2 amp. At this level, the regulator was sensitive to within a few tenths of a milliampere. A Rubicon type B potentiometer in conjunction with a Rubicon photoelectric galvanometer was used to make the emf measurements. Although the possible sensitivity of this arrangement was 0.1 μv, the actual sensitivity for the emf measurements was 0.5 μv due to noise in the rest of the circuit.

Most of the measurements were made at the constant temperatures of boiling liquids. In some cases for which a continuous increase in sample temperature was desired, isopentane was cooled to just above its freezing point and poured into the precooled Dewar which held the sample. The temperature of the isopentane increased at the rate of about 0.5 to 1.5°K per minute, depending on the amount of power dissipated by the sample.

Method for Measuring the Saturation Magnetization of Uranium Monosulfide

A comparison method was devised to determine the saturation magnetization I_S of US. The method was based on the fact that in a coin-shaped cavity in a magnetic material the force experienced by a moving

test charge is due entirely to the magnetic induction in the material. A coin-shaped cavity was simulated by bringing the ends of two cylinders close together, and the field measured in this gap was designated the effective induction B_{eff}. The saturation value of the effective induction obtained with cylinders made of nickel was compared with the value obtained with cylinders made of US. With a known value of I_s for nickel it was possible to determine the value of I_s for US. The method is described in detail below.

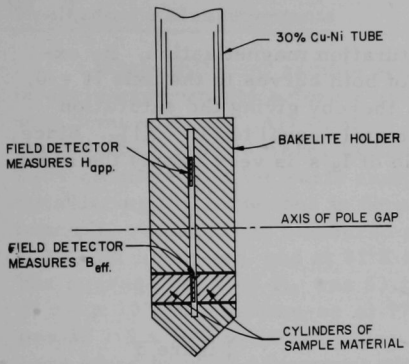

Figure 2. Sample Holder Used in Making Magnetic Measurements

Figure 2 illustrates the apparatus used in this experiment. The effective induction between the two cylinders was determined by measuring the Hall emf of the calibrated field detector between the cylinders. Another field detector in the same plane as the first, but away from the gap between the cylinders, measured the applied field. Since the gap between the two cylinders was narrow as compared with the sizes of the cylinders, the magnitude of B_{eff} measured in the gap was very nearly the same as the magnitude of the magnetic induction B in the material.

For cylindrical geometry, the induction in the material is related to the applied field by

$$B_{eff} \approx B = H_{app} + (4\pi - N)\, I \quad , \qquad (2)$$

where N is the demagnetization factor associated with the demagnetizing field due to the poles formed on the outer faces of the cylinders. According to Bozorth,[2] cylinders in which the ratio of long to short axis is small have a value of N associated with them which is only slightly dependent on the permeability of the material of which the cylinder is composed. The ratio of the long to short axis in the cylinders used for this experiment was 1.5, and the value of N for this ratio was constant to within 2 per cent if the permeability varied from 0 to ∞. Thus, through use of cylinders of identical size, the demagnetizing factor was assumed constant for the various materials compared.

When the assembly in Figure 2 was placed in the gap of the magnet, curves of B_{eff} versus H_{app} as in Figure 3 were obtained. It was observed

that for sufficiently high fields the induction varied linearly with the field. In this region equation (2) reduces to

$$B_{eff} \approx B = H_{app} + (4\pi - N) I_s \quad , \tag{3}$$

where I_s is constant and equal to the saturation magnetization. By extrapolation of the straight-line portions of both curves to the axis H = 0, the vertical intercepts were determined, thereby giving the saturation value of B_{eff} for each material, approximately equal to $(4\pi - N) I_s$. Since N is the same for all materials, the ratio of I_s's is very nearly the same as the ratio of B_{eff}'s.

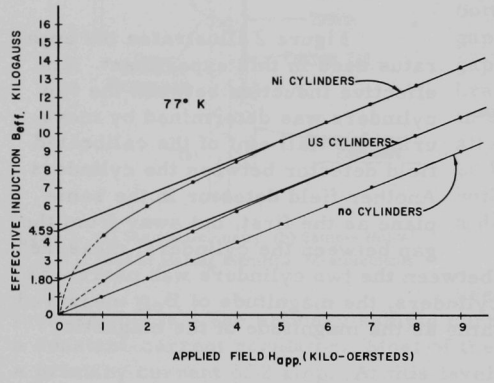

Figure 3

Effective Induction versus Applied Field at 77°K for Ni and US

In Figure 3, the curve obtained without cylinders in the apparatus served as a base line to determine when saturation had been reached. If saturation had not been reached, the line drawn through the experimentally determined points would not be parallel with the base line. This deviation was observed during an attempt to determine the accuracy of the method by comparing nickel with iron. Since the saturation magnetization of iron is considerably higher than that of nickel and since the maximum applied field was only 14.0 koe, it was not possible to saturate the iron completely.

The measured value of I_s for iron was 1,580 ± 60 cgs units at 300°K. This is to be compared with the value of 1,720 cgs units reported in the International Critical Tables.[18]

CHAPTER III

EXPERIMENTAL RESULTS

Preliminary Measurements

Eight different sample preparations of polycrystalline US were used in early experiments before a complete set of measurements was obtained with Sample P-109. Arc-melted and sintered samples were used. More reproducible results were obtained with the sintered samples. The results obtained with the early samples showed a reasonable consistency considering the variations in density and chemical composition. For example, resistivities measured at 300°K had an average value of 440 ± 120 μohm-cm, and at 77°K the average value was 180 ± 60 μohm-cm. The average value of R_0 was 53 ± 5 x 10^{-12} v-cm/amp-oe at 300°K and 27 ± 2 x 10^{-12} v-cm/amp-oe at 77°K. The average value of R_1 at 77°K was 32 ± 8 x 10^{-9} v-cm/amp-oe. All of the preliminary measurements were found to be in agreement with the detailed measurements reported in the following sections.

The Resistivity and Magnetoresistance of Uranium Monosulfide

The resistivity of US was measured at various temperatures, and the results are given in Table 3. The curve in Figure 4, obtained for Sample P-109, indicates the variation of resistivity with temperature. Measurements made at the temperatures of boiling liquids are represented as points on this curve. The shape of the resistivity versus temperature curve was qualitatively the same for Sample P-72.

Table 3. Data Describing Magnetic and Electrical Properties of Uranium Monosulfide

Temperature, °K	Effective Induction Intercepts			Saturation Magnetization I_S, gauss		Resistivity ρ, μohm-cm	Hall Mobility, μ_H	Effective Number of Carriers Per Atom	Hall Coefficients		
	Ni	US	Ni/US	Ni	US				$R_0 \times 10^{12}$, $\frac{\text{v-cm}}{\text{amp-oe}}$	Intercept, $\frac{\mu\text{v-cm}}{\text{amp}}$	$R_1 \times 10^9$, $\frac{\text{v-cm}}{\text{amp-oe}}$
4.2					210	106	6.1	0.45	6.5	2.10	9.99
77	4.59	1.80	2.55	523	205	174	16.1	0.105	28	6.83	33.3
112	4.54	1.75	2.59	502	194	243	18.9	0.064	46	13.8	71.0
169	4.42	1.16	3.81	495	130	398	26.6	0.028	106	25.4	195.0
185						474	103	0.006	495		
233						501	27.9	0.021	140		
263						505	16.0	0.036	81		
300						523	10.7	0.053	56		
363						541	7.0	0.077	38		

Particular emphasis was placed on measurements in the vicinity of the Curie point. The dashed curve in Figure 4 was obtained by making resistivity measurements while the temperature of the sample was increasing.

A slow continuous increase in sample temperature was accomplished by allowing the cooled liquid in which the sample was immersed to warm up. Temperature gradients may exist in such liquids and, since the sample and its lead wires form a thermocouple, a difference in temperature between the sample tabs could very possibly introduce an emf due to the Seebeck effect, which could account for the difference between the dashed and solid curves. The shape of the dashed curve indicates the approximate position of the Curie point.

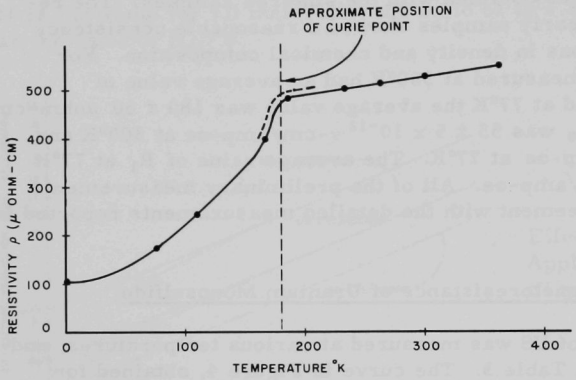

Figure 4

Temperature Dependence of Resistivity of US

The transverse magnetoresistance was measured as a function of temperature with various applied fields. Typical results for an applied field of 20 koe, illustrated in Figure 5, were obtained with Sample P-109. The measurements near the Curie point were made as the sample temperature was continuously increasing. It should be noted that the magnetoresistance is negative and has a very sharp minimum at the Curie point.

The transverse magnetoresistance of P-109 was also measured as a function of applied field at constant temperatures. Figure 6 indicates a linear dependence of magnetoresistance on field, above saturation at 169°K and at 185°K. The measurements at 185°K are more reliable than those at 169°K because above the Curie point the zero-field resistivity is not as sensitive to temperature as it is below the Curie point. At fields large enough to saturate

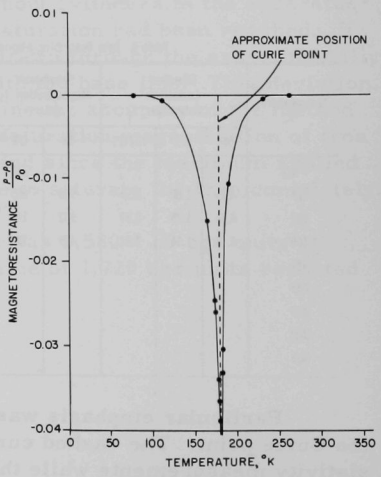

Figure 5. Transverse Magnetoresistance of US versus Temperature at 20 koe

the material, the magnetoresistance was the same for both directions of field. At low fields below the Curie point, the magnetoresistance displayed a hysteresis with field, but the exact nature of this hysteresis was not determined.

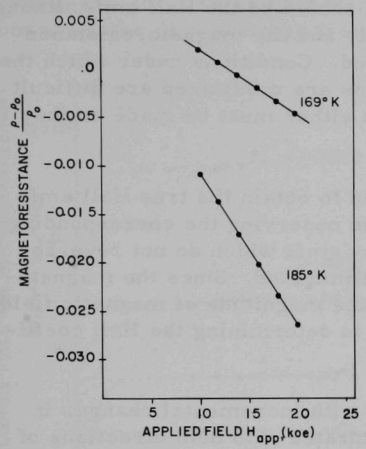

Figure 6. Transverse Magnetoresistance of US versus Applied Field at 169 and 185°K

The Saturation Magnetization of Uranium Monosulfide

The saturation magnetization I_S of US was determined at various fixed temperatures by the method outlined in Chapter II. The set of curves in Figure 3 represents the data used in determining I_S of US at 77°K for P-109 material. Values of I_S at various temperatures appear in Table 3 with the pertinent data from which these values were obtained.

The variation of I_S with temperature is indicated in Figure 7. The points plotted on this curve were taken directly from the experimental measurements reported in Table 3. The Curie point indicated was obtained from the magnetoresistance versus temperature curve in Figure 5. The value of I_0, the saturation magnetization at absolute zero, was obtained by extrapolation, using the limit of the Brillouin function for $J = \frac{1}{2}$:

$$I_S/I_0 = \tanh \frac{I_S/I_0}{T/\theta} \quad , \qquad (4)$$

where T is a given temperature, I_S is the saturation magnetization at that temperature, and θ is the Curie temperature.

The variation of I_S in the immediate vicinity of the Curie point has not been determined in this investigation. There is reason to believe that some saturation magnetization may exist above the Curie point. The significance of this will be discussed further below.

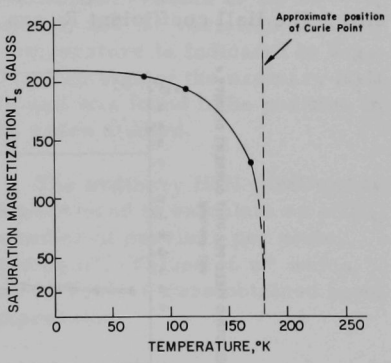

Figure 7. Saturation Magnetization of US versus Temperature

The Hall Effect in Uranium Monosulfide

The emf measured across tabs A and B in Figure 1(a) has at least three components. The largest component should be the Hall emf, although contributions from the zero-field resistivity and the magnetoresistance due to misalignment of the tabs are expected. Conditions under which the resistive and magnetoresistive contributions are minimized are difficult to obtain, and corrections for these effects either must be made or they must be eliminated experimentally.

One method which is commonly used to obtain the true Hall emfs consists of reversing the magnetic field and observing the corresponding changes in emf. Under these conditions any emfs which do not reverse with reversal of field are experimentally eliminated. Since the magnetoresistance of US depends only on the absolute magnitude of magnetic field above saturation, this method was utilized in determining the Hall coefficients of US.

The Hall emfs were also measured with incremental changes in field on a sample which was previously saturated with both directions of field. The data obtained in this way display a hysteresis of Hall emf with field. A curve of ϵ versus H_{app} at 77°K for Sample P-72 is illustrated in Figure 8. The uncorrected Hall emfs were used to plot these data, and the magnitude of the component of emf due to misalignment of tabs is indicated by the line which crosses the figure at 2.5×10^{-6} v-cm/amp. A careful study of Figure 8 indicates that above saturation the straight line obtained with positive field has a slope that is different from that of the line obtained with negative field. This difference can presumably be accounted for by considering the effect of the magnetoresistive component of emf. The Hall coefficient R_0 can be obtained by averaging these slopes.

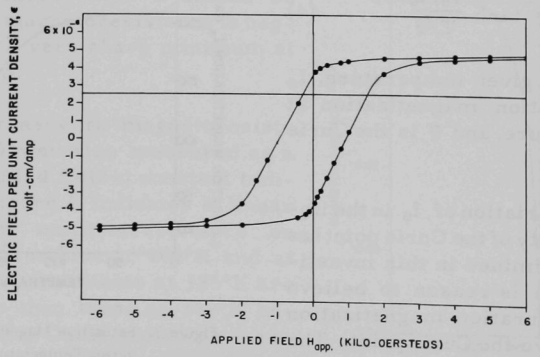

Figure 8. Electric Field Per Unit Current Density versus Applied Field at 77°K

The Hall coefficients reported here were obtained by using the first method exclusively. Curves of ϵ versus H_{app} were obtained for temperatures below and above the Curie point and are illustrated in Figures 9 and 10. The results were obtained from measurements of P-109; however, the data obtained from P-72 yielded similar results.

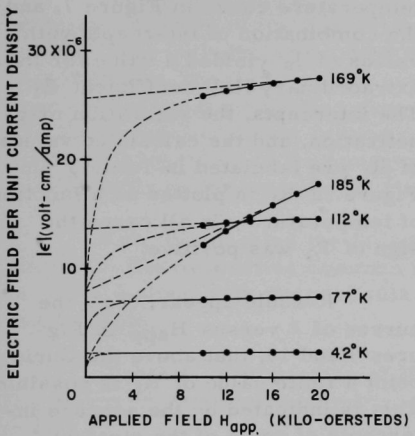

Figure 9. Electric Field Per Unit Current Density versus Applied Field at Low Temperatures

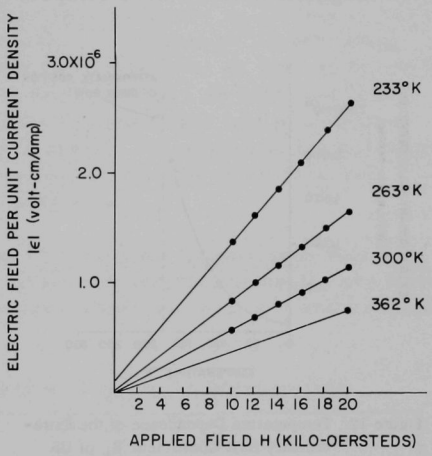

Figure 10. Electric Field Per Unit Current Density versus Applied Field at High Temperatures

The slope of the straight line portion of the ϵ versus H_{app} curve yields a value of R_0, the ordinary Hall coefficient. Values of R_0 at various temperatures are tabulated in Table 3, and the variation of R_0 with temperature is indicated in Figure 11. The sign of the ordinary Hall coefficient was found to be positive in all the cases studied.

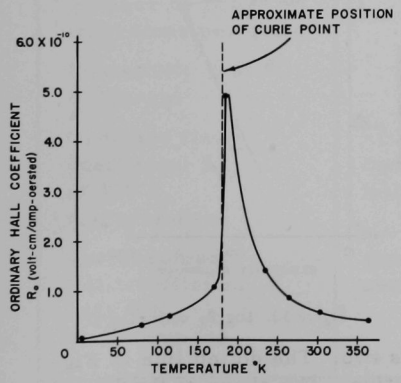

Figure 11. Temperature Dependence of the Ordinary Hall Coefficient R_0 of US

The ordinary Hall coefficients of US were used to calculate an effective number of carriers per atom, denoted by n*. Values of n* which appear in Table 3 were obtained from the expression .

$$n^* = -1/NR_0ec \quad , \qquad (5)$$

where N is the number of atoms/cc, e the electronic charge, and c the velocity of light. Since the electronic

charge has a negative sign associated with it and R_0 is positive, the values of n* are positive. The Hall mobilities μ_H are also given in Table 3.

The intercepts of the straight lines in Figures 9 and 10 with the axis H = 0, were determined for each temperature. Values of the saturation magnetization at these temperatures were obtained from the I_s versus temperature curve in Figure 7, and the combination of intercepts with values of I_s yielded a value for the extraordinary Hall coefficient R_1. The intercepts, the saturation magnetization, and the calculated values of R_1 are tabulated in Table 3. In Figure 12 R_1 is plotted as a function of temperature. In all cases the sign of R_1 was positive.

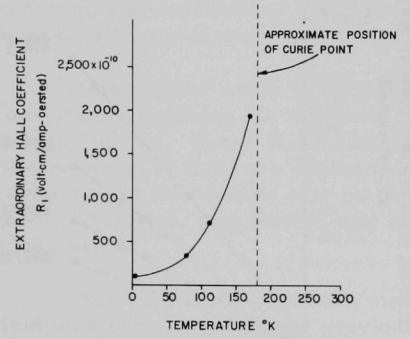

Figure 12. Temperature Dependence of the Extraordinary Hall Coefficient R_1 of US

It would appear, from the curves of ϵ versus H_{app} in Figures 9 and 10, that above the Curie point a finite value of R_1 is possible. This is indicated by the nonzero intercepts of some of the straight lines obtained above the Curie point. To account for a nonzero intercept above the Curie point, the saturation magnetization above the Curie point must have a nonzero value. This possibility has not been excluded, but before any definite conclusions can be made a more extensive investigation of the behavior of I_s with temperature would be necessary.

In Figure 13, log R_1 is plotted against log ρ. The points indicated in this figure were obtained from the measurements of the extraordinary Hall coefficients and the resistivities at various constant temperatures. Karplus and Luttinger[13] predicted that, for any ferromagnetic material,

$$R_1 = a\rho^b \quad , \qquad (6)$$

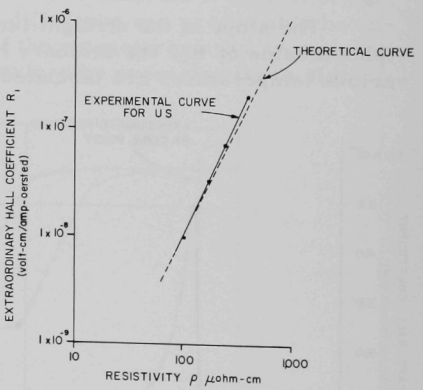

Figure 13. Log R_1 versus Log ρ

where a is of the order of unity and b is two. The dotted line in Figure 13 represents this theoretical prediction. The shape of the line obtained from the data with US indicates that a = 4 and that b = 2.15.

CHAPTER IV

DISCUSSION OF RESULTS

Comparison of Uranium Monosulfide with Other Ferromagnetic Materials

The comparison of US with other ferromagnetic materials is based on an examination of the properties which are common to all ferromagnetics. This includes properties above the Curie point as well as below it. Unfortunately, the Curie points of iron and cobalt are so high that measurements of most properties above these temperatures are prohibitive. The Curie point of nickel is lower; as a result, the studies of the galvanomagnetic properties of ferromagnetics reported in the literature rely quite heavily on measurements made with nickel.

With this in mind the following criterion for comparison was adopted. The properties common to all ferromagnetic materials are listed in Table 4 along with the particular values observed in nickel and uranium monosulfide.

Table 4. Comparison of Nickel with Uranium Monosulfide

Property	Nickel[2,10]	Polycrystalline Uranium Monosulfide (Sample P-109)
Curie point θ, °K	631	180
Saturation magnetization I_0 at 0°K, gauss	508.8	210 ± 5
Number of Bohr magnetons per atom	0.604	1.05 ± 0.03
Resistivity ρ at θ, μohm-cm	33	475 ± 10
Ordinary Hall coefficient R_0 at 300°K, v-cm/amp-oe	-0.611×10^{-12}; constant with temperature	56×10^{-12}; varies with temperature
Extraordinary Hall coefficient, R_1 near 0°K, v-cm/amp-oe	approaches zero	approaches 1×10^{-8}

Consider the magnetic properties first. The Curie point of US is lower than that of nickel; however dysprosium, CoS_2, AgF_2, and other materials have Curie points which are lower than that of US. UH_3 is ferromagnetic[19] and has a Curie point very close to that of US. Trzebiatowski and Suski[20] discovered a ferromagnetic transition in USe very recently and report a Curie point in the range 185-190°K. There is an interesting similarity between US and USe in that both have a cubic structure and both involve U^{++} in their composition.

The value of the saturation magnetization of US at absolute zero is comparable with that of other materials. The atomic moment for US derived from this quantity is approximately one Bohr magneton, which is very close to the values reported for UH_3 and USe. The shape of the I_s versus T curve in Figure 7 is similar to the shape of curves obtained for nickel, iron, and cobalt.[2] If these curves were drawn on a reduced scheme so that the values of I_0 and θ coincided for all the materials, the curve for US would be slightly higher than the others.

Although the resistivity of nickel is lower by an order of magnitude than that of US at an equivalent temperature, the resistivities of both materials display a similar temperature dependence, and the resistivity versus temperature curve in Figure 4 is typical of those observed in most ferromagnetics. The slope of the straight line obtained above the Curie point is usually greater in other ferromagnetic metals than it is in US.

The magnetoresistance versus temperature curve of Figure 5 is also similar to data obtained for nickel.[2] A minimum in magnetoresistance occurs at the approximate position of the Curie point for both materials. It should be pointed out, however, that the US curve has a much sharper minimum, i.e., the magnetoresistance increases to zero in a much smaller temperature range around the Curie point. The variation of magnetoresistance with field indicated in Figure 6 is in good agreement with the observations of Englert[21] for the transverse magnetoresistance of nickel wire.

The ordinary Hall coefficients R_0 of the common ferromagnetic metals are believed to be essentially constant in the entire temperature range except in the immediate vicinity of the Curie point. The sign of R_0 is negative for nickel and cobalt but positive for iron.[22] The absolute magnitude of R_0 is of the order of 0.5×10^{-12} v-cm/amp-oe. In comparison, R_0 of US has the temperature dependence indicated in Figure 11, has a positive sign, and has absolute magnitudes ranging from 7×10^{-12} to 5×10^{-10} v-cm/amp-oe.

It is likely that very close to the Curie point the measured value of R_0 cannot be interpreted in terms of an effective number of carriers. Since the magnetization can change with field in this region, even above

saturation, a contribution from R_1 would increase the slope of the ϵ versus H_{app} curves in Figures 9 and 10. In nickel this anomalous behavior of R_0 can exist within a temperature range of $\theta \pm 10$ per cent of θ. It is apparent from Figure 11 that, even if this range is somewhat greater in US, a maximum in the true R_0 would occur somewhere in the vicinity of the Curie point.

The temperature dependence of the extraordinary Hall coefficient R_1 of US, indicated in Figure 12, is similar to that of the other ferromagnetic materials. R_1 of US is positive and is approximately two hundred times larger than the values for iron, nickel, and cobalt at equivalent temperatures. The sign of R_1 of iron and cobalt is positive, while that of nickel is negative.

The dependence of R_1 of US on resistivity is in good qualitative agreement with the theoretical prediction, as is evidenced by the curves in Figure 13. It is interesting that quantitative agreement with theory is also observed in the data for iron, whereas data for nickel agree only qualitatively. The similarity between the properties of US and those of the ferromagnetic transition metals justifies an examination of the band structure adopted for the latter.

Discussion of the Band Model for Ferromagnetic Transition Metals

The electronic configurations of the transition metals lead to a band picture which consists of a broad 4s-band and a broad 3d-band with narrow regions of high density of states. From low-temperature specific heat data[23] it is known that the 3d-band consists of three sub-bands which can be related to a bonding doublet which has paired spins and an antibonding triplet which is split by a magnetic field below the Curie point and accommodates three electrons per atom with parallel spins in the lower half and three electrons per atom with antiparallel spins in the upper half.

To explain the low-temperature specific heats of iron, cobalt, and nickel, it is assumed that the lower half of the split 3d-triplet is completely filled.[24] Since the orbital contribution to the magnetic moment is found to be quenched in the transition metals, the atomic moment expressed in Bohr magnetons per atom must be equal to the number of unoccupied levels per atom in the upper half of the split 3d-triplet. Nickel, for example, has ten electrons which are distributed among the 3d- and the 4s-bands. Four of the electrons fill the bonding doublet, three of the electrons completely fill the lower half of the 3d-triplet, and to account for the 0.6 Bohr magneton per atom of nickel, 2.4 of the electrons must be in the upper half of the 3d-triplet. The remaining 0.6 electron per atom is in the 4s-band.

The Hall effect measurements with nickel[10] are consistent with the band picture to the extent that the ordinary Hall coefficient is negative,

indicating conduction by electrons. The predicted magnitude of the number of carriers per atom, 1.16, is too large if conduction is assumed to take place entirely in the 4s-band. A necessary consequence of this observation is that conductivity in the d-band is not negligible and does indeed contribute to the Hall effect.

If it is assumed that both the 3d- and the 4s-bands contribute to conduction, R_0 for the simple two-band model is given by[22]

$$R_0 = \frac{1}{Nn^*ec} = -\left\{\frac{1}{n_s}\left(\frac{\sigma_s}{\sigma}\right)^2 \pm \frac{1}{n_d}\left(\frac{\sigma_d}{\sigma}\right)^2\right\} \Big/ Nec \quad , \tag{7}$$

where n_s is the number of electrons per atom in the 4s-band, and n_d is either the number of holes per atom in a nearly filled 3d-band or the number of electrons per atom in a nearly empty 3d-band. The negative sign is chosen for holes and the positive sign for electrons. The total conductivity is designated by σ, and the conductivities of the 4s-band and 3d-band are designated by σ_s and σ_d, respectively.

Foner and Pugh[21] conclude that equation (7) accounts for values of n^* that are large compared with n_s and cannot account for n^* smaller than n_s unless $\sigma_d \gg \sigma_s$, which seems improbable. The best agreement with the results observed with nickel is obtained when n_d is taken for positive carriers and $\sigma_s > \sigma_d$. If $n_s = n_d = 0.6$ and $n^* = 1.16$, equation (7) gives $\sigma_d/\sigma_s = 0.3$.

Possible Band Model for the Actinide Sulfides

The interpretation of the data reported here is clearly quite speculative in that little is known about the energy levels in the actinide series of elements and one must look to the transition metals for guidance.

In adapting a band picture to the observed phenomena in US, the core electrons can be disregarded. The levels to be considered are $(7s)^2(5f)^3(6d)^1$ for uranium and $(3p)^4$ for sulfur. It seems reasonable that two electrons from uranium fill the 3p-band of sulfur; this would tend to lower the levels in sulfur and raise those of uranium. Since the 3p-band is full, it can be disregarded as are the core electrons. The remaining four electrons must then be distributed among a band formed by the 7s-levels, which would be broad, and the bands of 5f- and/or 6d-levels which are expected to contain narrow regions of high density of states.

A band picture must be consistent with the following observations:

1. US is ferromagnetic and the magnetic moment/atom at 0°K is 1.05 Bohr magnetons/atom.

2. The resistivity below the Curie point is abnormally low.

3. The magnetoresistance is low in the entire temperature range except for a sharp minimum at the Curie point.

4. The ordinary Hall coefficient is temperature dependent with an apparent maximum near the Curie point and has a positive sign.

The analogy with the transition metals, in which the d-band is split into a lower bonding doublet which has paired spins and an anti-bonding triplet which gives rise to the magnetic moment, would seem to rule out an explanation which involves s- and d-bands only. With four electrons, only the paired spin states in the lower bonding sub-bands can be filled, which would make it impossible to explain the ferromagnetic behavior of US.

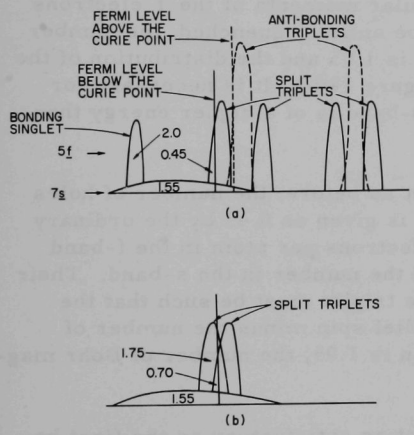

Figure 14. Possible Band Structures for US (a) Assuming Orbital Momenta are not Quenched, (b) Assuming Orbital Momenta are Quenched

The picture based on overlapping f and s orbitals seems somewhat more promising. The f-levels in cubic symmetry are split into a singlet level and two triplet levels.(25) This leads to the simple band picture shown in Figure 14(a).

If the orbital contribution to the magnetic moment is not quenched, an electron in the antibonding triplet state may contribute more than one Bohr magneton per atom to the atomic moment. Since f electrons probably do not take part in chemical bonding in the actinides, it is reasonable to assume that the orbital contribution is not quenched, and the difference between the parallel and antiparallel spin electrons could be less than 1.05 electrons per atom.

If it is assumed that the conductivity is due mostly to the holes in the s-band, then the number of holes per atom at absolute zero in this band is the effective number derived from the Hall coefficient. The distribution of the electrons among the two bands would be that illustrated in Figure 14(a) with possible variations in the occupation of the triplet sub-bands.

The band picture depicted in Figure 14(a) is one possible way of describing the electronic distribution which explains the experimental data. The picture indicated by the solid lines describes the situation at absolute zero, where US is ferromagnetic and the measured atomic moment of

1.05 Bohr magnetons per atom arises from 0.45 electron per atom with spins parallel. As the temperature is increased above absolute zero, the halves of the split triplet sub-bands move toward their centers of symmetry, and above the Curie point they each form single sub-bands, as indicated by the dotted lines. It is apparent that the number of holes in the 4s-band would decrease with increasing temperature up to the Curie point and that somewhere in the vicinity of the Curie point this number would start increasing with increasing temperature. This is consistent with the observed temperature dependence of the ordinary Hall coefficient. Similar to the case of other ferromagnetic materials, the temperature dependence of resistivity and magnetoresistance could be explained on the basis of a decrease in s-f transitions below the Curie point due to the splitting into parallel and antiparallel states.

If the contribution of orbital angular momenta of the f electrons to the magnetic moment is assumed to be entirely quenched, the number of electrons contributing to the moment is 1.05 and the distribution of the four electrons in US is illustrated in Figure 14(b). It is necessary for this configuration that the 5f singlet sub-band is of a higher energy than one of the triplets.

If the 4s conductivity is dominant as before, the number of holes per atom in the s-band at absolute zero is given as 0.45 by the ordinary Hall coefficient. The total number of electrons per atom in the f-band must be the difference between four and the number in the s-band. Their distribution in the two split halves of the triplet must be such that the number of electrons per atom with parallel spin minus the number of electrons per atom with antiparallel spin is 1.05, the number of Bohr magnetons per atom.

The second case illustrated is not as satisfactory as the first because, without a more detailed knowledge of the bands involved, it is difficult to compare the expected temperature dependencies with those observed. It should not be excluded, however, as one of the possible band models for the actinide sulfides, at least not on the basis of the results of this research.

Conductivity in the f-bands is not completely ruled out by these experiments. Minor conductivity by carriers of low mobility would not affect the qualitative picture given here; however, any major conductivity in the f-bands would imply a very much larger mobility for f-band carriers than for s-band carriers. The two alternative band pictures given here are considered to be more probable. It should be pointed out that additional models may exist which involve mixtures of s-, f-, and d-bands.

Further research on the actinide sulfides is intended, and one approach already considered is to study solid solutions of US and ThS. Since ThS has two electrons fewer than US and is not ferromagnetic, it is anticipated that, if the band model in Figure 14(a) is representative of the

electronic structure of these sulfides, US-ThS solid solutions will be non-ferromagnetic above approximately thirty per cent of the ThS phase.

Extension of these studies to materials such as UP, UC, USe, UAs, and others is also under consideration. All of these compounds have the same crystal structure, a metallic appearance, high conductivity, and numerous other interesting properties. In addition to galvanomagnetic studies, low-temperature specific heat, susceptibility, and neutron diffraction studies would be useful in arriving at a thorough understanding of 7s-5f electronic structures in these compounds.

CHAPTER V

SUMMARY

The magnetic and galvanomagnetic properties of uranium monosulfide, including resistivity, magnetoresistance, and Hall effect, were studied. The resistivity was found to be approximately a hundred times higher in US than in the common ferromagnetic metals, but the temperature dependence of resistivity was similar, showing an abnormal decrease below the Curie point. The magnetoresistance of US was found to be negative with a sharp minimum at the Curie point. The study of the Hall effect revealed that two Hall coefficients could be identified. The extraordinary Hall coefficient, which is related to the magnetization of the material, was found to be proportional to the second power of the resistivity. The ordinary Hall coefficient R_0, related to the applied field, was found to be positive and temperature dependent, with a maximum near the Curie point. The temperature dependence of R_0 constituted the biggest dissimilarity between US and other ferromagnetic substances. The effective carrier concentration evaluated from this coefficient was 0.45 hole per atom at absolute zero. The study of the magnetic properties yielded values of the saturation magnetization at various temperatures which indicated that at absolute zero the atomic moment is 1.05 ± 0.03 Bohr magnetons. These results have been correlated with a band picture based on overlapping 7s and 5f bands.

BIBLIOGRAPHY

1. Kanter, M. A., and C. Kazmierowicz, Bull. Am. Phys. Soc. Ser. II, 7 (1962) 556.

2. Bozorth, Richard M., Ferromagnetism. D. Van Nostrand Company, Inc., New York (1953).

3. Becker, R., and W. Doring, Ferromagnetismus. Springer, Berlin (1939).

4. Mott, N. F., Proc. Roy. Soc. (London) 153A 699 (1936).

5. Gerlach, W., Physik, Z., 59 847 (1930).

6. Smith, A. W., Phys. Rev. 30 1 (1910).

7. Pugh, E. M., Phys. Rev. 32 824 (1928).

8. Pugh, E. M., Phys. Rev. 36 1503 (1930).

9. Pugh, E. M., and T. W. Lippert, Phys. Rev. 42 709 (1932).

10. Pugh, E. M., N. Rostoker, and A. Schindler, Phys. Rev. 80 688 (1950).

11. Jan, J. P., and H. M. Gipman, Physica 5 277 (1952).

12. Rostoker, N., and E. M. Pugh, Phys. Rev. 82 125 (1951).

13. Karplus, R., and J. M. Luttinger, Phys. Rev. 95 1154 (1954).

14. Kooi, C., Phys. Rev. 95 843 (1954).

15. Schindler, A. I., and E. I. Salkovitz, Phys. Rev. 99 1251 (1955).

16. Jellinghaus, W., and M. P. De Andres, Ann. Phys. 1 189 (1961).

17. Cater, E. D., P. W. Gilles, and R. J. Thorn, J. Chem. Phys. 35 608 (1961).

18. West, C. J., International Critical Tables of Numerical Data. McGraw-Hill Book Company, Inc., New York and London (1933).

19. Gruen, D. M., J. Chem. Phys. 23 1708 (1955).

20. Trzebiatowski, W., and W. Suski, Bull. Acad. Polon. Sci. Chim. 10 399-400 (1962).

21. Englert, E., Ann. Physik 14 589 (1932).

22. Foner, S., and E. M. Pugh, Phys. Rev. 91 20 (1953).

23. Cheng, C. H., C. T. Wei, and P. A. Beck, Phys. Rev. 120 426 (1960).

24. Seitz, F., The Modern Theory of Solids. McGraw-Hill Book Company, Inc., New York and London (1940).

25. Jorgensen, C. K., Absorption Spectra and Chemical Bonding in Complexes. Addison-Wesley Publishing Company, Inc., Reading, Mass. (1962).

ACKNOWLEDGEMENT

The author expresses his sincere thanks to the Physics Department Staff of IIT for making it possible to apply this work toward partial fulfillment of the requirements for the degree of Master of Science in Physics and to Dr. O. C. Simpson, Director of the Solid State Science Division of Argonne for his cooperation.

Further thanks and sincere appreciation is extended to Dr. Manuel A. Kanter for his suggestion of the problem, his guidance in making the measurements, and the many helpful discussions leading to the ultimate interpretation of the results. Thanks are also extended to Professor Leonard Grossweiner for his advice and encouragement during the course of the work.

The author is indebted to the members of the graphite group of the Solid State Science Division for certain research facilities. Acknowledgement is made to Dr. Marvin Tetenbaum and Mr. Peter Shalek of Argonne who provided the uranium monosulfide used in this research.

The research for this thesis was carried out at Argonne National Laboratory under the auspices of the United States Atomic Energy Commission.